INTERNATIONAL JOURNAL OF CLIMATOLOGY
Int. J. Climatol. **27**: 179–187 (2007)
Published online 10 October 2006 in Wiley InterScience
(www.interscience.wiley.com) DOI: 10.1002/joc.1394

RMetS
ROYAL METEOROLOGICAL SOCIETY

Indian summer monsoon rainfall and its link with ENSO and Indian Ocean climate indices

Chie Ihara,[a,*] Yochanan Kushnir,[a] Mark A. Cane[a] and Victor H. De La Peña[b]
[a] *Lamont-Doherty Earth Observatory of Columbia University, 61 Route 9W Palisades, NY 10964-8000, New York*
[b] *Department of Statistics, Columbia University, 1255 Amsterdam Avenue, NY 10027, New York*

Abstract:

We examine the relationship between the state of the equatorial Indian Ocean, ENSO, and the Indian summer monsoon rainfall using data from 1881 to 1998. The zonal wind anomalies and SST anomaly gradient over the equatorial Indian Ocean are used as indices that represent the condition of the Indian Ocean. Although the index defined by the zonal wind anomalies correlates poorly with Indian summer monsoon rainfall, the linear reconstruction of Indian summer monsoon rainfall on the basis of a multiple regression from the NINO3 and this wind index better specifies the Indian summer monsoon rainfall than the regression with only NINO3. Using contingency tables, we find that the negative association between the categories of Indian summer monsoon rainfall and the wind index is significant during warm years (El Niño) but not during cold years (La Niña). Composite maps of land precipitation also indicate that this relationship is significant during El Niño events. We conclude that there is a significant negative association between Indian summer monsoon rainfall and the zonal wind anomalies over the equatorial Indian Ocean during El Niño events. A similar investigation of the relationship between the SST index and Indian summer monsoon rainfall does not reveal a significant association. Copyright © 2006 Royal Meteorological Society

KEY WORDS Indian summer monsoon rainfall; ENSO; Indian Ocean Dipole Mode

Received 25 June 2005; Revised 25 March 2006; Accepted 27 June 2006

1. INTRODUCTION

The all-India summer monsoon rainfall (hereafter referred to as ISMR, Sontakke *et al*., 1993), is defined as the rainfall received during the summer monsoon season (June, July, August, and September) over India. The ISMR has a large impact on the agriculture and related economic activities of the region, and prediction of the interannual variability of ISMR is thus a matter of great concern to society. Researchers have been working on this problem since the late 1800s. El Niño and Southern Oscillation (ENSO) has been known to exert the most important external forcing on ISMR (e.g., Krishna Kumar *et al*., 1999; Rasmusson and Carpenter, 1983; Webster and Yang, 1992; Ropelewski and Halpert, 1987; Lau and Nath, 2000; Wang *et al*., 2003). As Walker found out long ago, the anomalous high pressure over the western Pacific–eastern Indian Ocean and anomalous low pressure over the eastern and central Pacific associated with El Niño, influence the monsoon circulation. Krishna Kumar *et al*. (1999), among others, suggest that El Niño/La Niña shifts the location of the tropical Walker circulation and brings about deficit/excess of rainfall by suppressing/enhancing the convection over the Indian region.

The canonical patterns of atmospheric and oceanic variables over the Indo Pacific regions during El Niño and La Niña events were described by Reason *et al*. (2000). They showed that when an El Niño occurred during the summer, the Indian Ocean was characterized by a slight warming of SST compared to normal, which was associated with weaker wind magnitudes than normal and reduced cloudiness. After the summer monsoon season, they found a clear influence of El Niño over the Indian Ocean; the SST over the entire basin was significantly warmer than normal. At this time, large negative wind speed anomalies around the equator were seen in the Indian Ocean, with an increase in cloudiness over the western Indian Ocean, and a decrease over the eastern Indian Ocean. They also demonstrated that the opposite configuration occurred during La Niña events.

The state of ENSO does not explain all the interannual variability of ISMR (Kripalani and Kulkarni, 1997). For example, in spite of the occurrence of strong El Niño events in 1914, 1963, 1976, 1983, and 1997, these years did not experience deficiencies in ISMR (Figure 1). Kripalani and Kulkarni (1997) pointed out the existence of the interdecadal variability of ISMR and found that when ISMR was in the above normal interdecadal phase,

* Correspondence to: Chie Ihara, Lamont-Doherty Earth Observatory of Columbia University, 61 Route 9W Palisades, NY 10964-8000, New York. E-mail: cihara@ldeo.columbia.edu

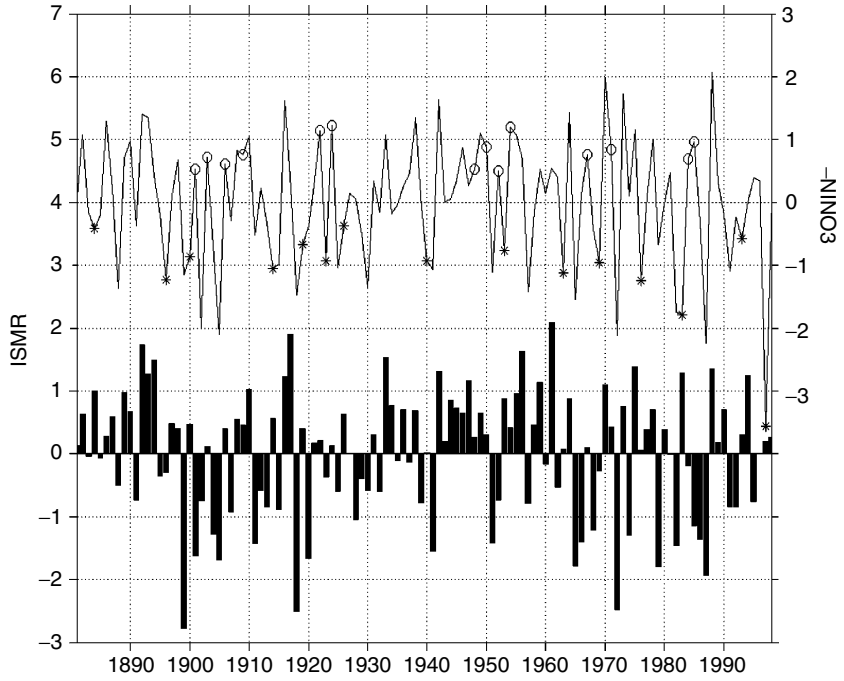

Figure 1. Time series of ISMR and −NINO3 from 1881 to 1998. Bars indicate ISMR and the line indicates −NINO3. The ISMR values of */o years do not fall in the lower/upper 33% of its distribution despite the occurrence of El Niño/La Niña.

even strong El Niño events did not bring severe droughts to India.

The link between the state of the Indian Ocean and interannual variability of ISMR has been investigated for the last three decades (Saha, 1970 and references in Kripalani *et al*., 2005). In particular, it is argued that the Indian Ocean Dipole (IOD) mode, which is generally identified on the basis of the SST anomaly difference between the western and eastern equatorial Indian Ocean (Saji *et al*., 1999; Webster *et al*., 1999), influences interannual ISMR variation. Ashok *et al*. (2001) demonstrated a complementary relationship between ENSO-ISMR and IOD-ISMR during the period of 1958–1997 from observational analysis and AGCM experiments. They claimed that when the ENSO-ISMR correlation is weak, the ISMR better correlates with IOD than when it is strong. More recently, they also found that a positive IOD state reduces the impact of ENSO on ISMR by inducing anomalous surface divergence in the eastern tropical Indian Ocean. At the same time, a positive IOD also directly influences the ISMR because the warm pole of the positive IOD in the western Indian Ocean is associated with an anomalous ascent over India and, thus, with surplus rainfall (Ashok *et al*., 2004).

Gadgil *et al*. (2003) found that the positive phase equatorial Indian Ocean Oscillation (EQUINOO), or the enhancement/reduction of convection in the western/eastern equatorial Indian Ocean (which might be the atmospheric component of the coupled IOD mode but is not always linked to the IOD SST anomalies) is linked with the ISMR, and that ENSO and EQUINOO together explain the ISMR variability during the period of 1979–2002. In their recent paper, Gadgil *et al*. (2004) found that a composite index formed as a linear combination of the EQUINOO zonal wind index (hereafter referred to as EQWIN) and the ENSO index, better correlates with a large excess or deficit in ISMR than either index alone. They also found that the large excess and deficit ISMR events are separated by a line determined by a linear combination of the EQWIN and ENSO index. They suggested the physical mechanisms of this link as the EQUINOO, i.e. the convection in the western Indian Ocean propagates northward and this propagation is associated with the enhancement of the large-scale monsoon rainfall over India.

Previous studies looking at the Indian Ocean-ISMR relationship were motivated by the weakening of the Monsoon-ENSO relationship in recent decades (Krishna Kumar *et al*., 1999), and thus the data that they analyzed were limited to this period. This raises a question whether the proposed relationship can hold over longer timescales. In this study, we examine the relationship between the state of equatorial Indian Ocean climate, ENSO, and ISMR using the ISMR record from 1881 to 1998 (Sontakke *et al*., 1993). Following the previous studies cited above, we particularly focus on the Dipole Mode Index obtained from SST (hereafter SSTDMI) and EQWIN as the indices that represent the condition of Indian Ocean climate. Because the linkage between SSTDMI/EQWIN and ISMR is weak, we use, in addition to regression analyzes, the robust method of contingency tables to quantify the relationship more clearly.

In Section 2, we describe the data sources. Section 3 is devoted to the results of various statistical analysis that demonstrate the relationship between ISMR, ENSO,

DOI: 10.1002/joc

and EQWIN. The summary and discussion are given in Section 4.

2. DATA DESCRIPTION

The following data sets are used in this study:

(1) Indian Summer Monsoon Rainfall (ISMR) record: the all-India summer monsoon rainfall during 1881–1998 is from Sontakke *et al*. (1993). Data is constructed by combining rainfall gauge observations at 36 stations distributed homogeneously over India.
(2) ENSO index: we use the so-called NINO3 index, i.e. the SST anomaly averaged over the region (90–150°W, 5°N–5°S). Monthly, gridded SST anomalies from Kaplan *et al*. (1998) are averaged over the indicated region. The data are then averaged over the summer monsoon season (June–September) and normalized. Data prior to 1880 are not included in our analysis to avoid the uncertainties that are reported to affect this early period (Kaplan *et al*., 1998).
(3) The Indian Ocean SST Dipole Mode Index (SSTDMI) is based on the SST anomaly difference between the western (52.5–67.5°E, 7.5°S–7.5°N) and eastern (92.5–107.5°E, 7.5–2.5°S) equatorial Indian Ocean. Here too the monthly, gridded SST anomalies during the period of 1881–1998 are obtained from Kaplan *et al*. (1998). For comparison, monthly gridded SST anomalies are also obtained from the Hadley Center HadISST data set (Rayner *et al*., 2003), which correlate well with the SSTDMI that is based on the Kaplan data (the correlation coefficient is 0.84 during the period of 1881–1998).

The time series of SSTDMI shows decadal variability; it tends to be on the negative side during the period prior to 1920 and positive thereafter (Kripalani and Kumar, 2004). Also, Indian Ocean SSTs display a clear warming trend during the analysis period, particularly in recent decades. We do not remove this trend or any other low-frequency signal from the data since we found that doing so does not significantly impact our results. The data are averaged over the summer monsoon season (June–September) and normalized.

The quality of the historical data over the tropics, particularly the tropical Pacific, and the effect on the resulting analysis are discussed in Kaplan *et al*. (1998). The data are richer over the Indian Ocean than in the Pacific. From 1881 to 1998, there are three short periods when the *in-situ* data are rather sparse over the Indian Ocean; before 1900s, during 1915–1920, and 1940–1945. Except for these, the number of observations over the SSTDMI region before 1950s is comparable to those even after 1980s. To further address the data quality, we repeated some of our analysis separating the data record into two segments (see below) and confirming that the results are not significantly different in the first and second half of the record.

(4) EQWIN is based on the zonal surface wind anomalies averaged over the equatorial Indian Ocean (62–90°E, 4°S–4°N). The monthly zonal wind anomalies during 1881–1998 are obtained from ICOADS (Worley *et al*., 2005). There is a trend in the zonal wind anomaly data, but the trend has little effect on our results. The data are averaged over the summer monsoon season (June–September) and normalized.
(5) Land precipitation data are obtained from Hulme (1992, 1994) and Hulme *et al*. (1998). As described in these references, they were reconstructed from historical monthly rain gauge observations over the global land areas and averaged on a 3.75 by 2.5 grid, from 1900 to 1998.

3. RESULTS

3.1. ISMR reconstruction from ENSO and Indian Ocean climate Indices

We used linear and non-linear statistical regression models to study the relationship between ISMR from the indices of the Pacific and Indian Oceans.

As the previous studies have discovered, there is a negative correlation between the ENSO indices and ISMR. The simultaneous correlation coefficients between the ENSO indices, such as NINO3/NINO3.4/NINO4 and ISMR are $-0.57/-0.59/-0.47$, respectively, using all the years from 1881 to 1998 (NINO3.4: mean SST anomaly over 120–170°W, 5°N–5°S. NINO4: mean SST anomaly over 150°W–160°E, 5°N–5°S). The NINO3.4 correlation with ISMR is almost identical to that of NINO3. Since the results are not sensitive to the choice of these indices, we adopted NINO3 as the ENSO index for this study.

The Indian Ocean is influenced by the seasonal evolution of ENSO. Reason *et al*. (2000) made composite maps of sea-level pressure, SST, wind and cloudiness anomalies for the various ENSO stages and showed that the changes in the cloud cover and winds caused by ENSO tended to generate SST response in the Indian Ocean. In this study we found that during the period analyzed, simultaneous correlation coefficients of NINO3 and SSTDMI/EQWIN are $0.39/-0.28$, respectively. Thus, the Indian Ocean indices of the monsoon season are only weakly dependent on the concomitant state of ENSO.

The correlations between the two Indian Ocean indices and ISMR are poor. The simultaneous correlation coefficients of SSTDMI or EQWIN with ISMR are -0.16 and -0.15, respectively; thus the connections between the state of Indian Ocean climate indices and ISMR are weak when measured over the long interval 1881–1998 and quantifying the relationship by the usual regression analysis would be a futile exercise. However, we are interested in finding out what information, additional to that determined by the state of ENSO, can be gleaned from the state of the Indian Ocean.

Table I summarizes results from four different ISMR reconstruction models obtained by linear and non-linear multiple regressions. In model 1, the ISMR is reconstructed from the NINO3 index alone. Models 2 and 3

DOI: 10.1002/joc

Table I. The results from the four different ISMR reconstruction models obtained by linear and non-linear multiple regressions. AIC, the Akaike Information Criterion, is calculated for each model.

Model No.	Explanatory variables	Multiple correlation coefficient	Model equation	AIC
1	NINO3	0.57	ISMR = $-0.57 \times$ NINO3	175
2	NINO3, EQWIN	0.66	ISMR = $-0.67 \times$ NINO3 $-0.34 \times$ EQWIN	156
3	NINO3, SSTDMI	0.57	ISMR = $-0.6 \times$ NINO3 $+0.07 \times$ SSTDMI	176
4	NINO3, EQWIN, NINO3 $\times$ EQWIN	0.69	ISMR = $-0.73 \times$ NINO3 $-0.33 \times$ EQWIN $-0.19 \times$ EQWIN $\times$ NINO3 $- 0.05$	146

are based on the multiple regressions of ISMR on the NINO3 and EQWIN indices and the NINO3 and SSTDMI indices, respectively. The fourth model is based on the NINO3 and EQWIN indices and includes a non-linear term defined as the product of these indices, which measures the influence of the co-occurrence of large EQWIN and NINO3 on ISMR.

The linear reconstruction of ISMR on the basis of both the ENSO index and EQWIN (model 2) has a stronger correlation with the observed ISMR than the NINO3 only regression (model 1). The overall correlation between the reconstructed ISMR by model 2 and the true ISMR is 0.66 (95% confidence interval is $0.54 < r < 0.75$).

The reconstruction of ISMR that includes a non-linear term (model 4) correlates with ISMR more strongly than model 1 and 3, and as strong as model 2, with a correlation coefficient of 0.69 (95% confidence interval is $0.58 < r < 0.77$). The linear combination of EQWIN and NINO3 explains about 44% of the variance of the ISMR and the composite index that includes a non-linear term explains 49%, while the NINO3 index alone explains only 32% of the variance. In contrast, a model akin to model 2, which uses SSTDMI as the index of the Indian Ocean instead of EQWIN, does not improve the correlation coefficient with the true ISMR over that obtained with NINO3 alone. Thus, while wind information helps, no skill is added to the specification of ISMR by the SSTDMI index when analyzed over the long interval from 1881 to 1998.

As the number of explanatory variables increases, the degree of freedom of the model decreases. Thus, we calculated the Akaike Information Criterion (AIC) values, which take this fact into account to select the best model from the four described above (Sakamoto *et al*., 1986). The smaller the AIC is, the better the model reconstructs ISMR, and comparing AIC values gives the optimum model. In practice, when the difference in AIC values between two models is greater than 10, the model with larger AIC values is significantly inferior to the one with the smaller AIC value (Burnham and Anderson, 2003). In this analysis, AIC values rank from the smallest for model 4 to the largest for model 3. Since the AIC value of model 2 is smaller than that of model 1 by 19, we conclude that adding EQWIN significantly improves the specification of ISMR from that based on ENSO only. Since model 4 has the minimum AIC value, smaller than that of model 2 by 10, the non-linear regression that includes the ENSO index, EQWIN, and their products improves ISMR reconstruction. This term indicates the importance of the influence of EQWIN when it is strong (>1).

The multiple regression analysis described above was performed separately with the fist and second half of the record (1881–1949 and 1950–1998). The results in the two segments were consistent with one another and did not differ in any significant way, confirming that the data are reliable throughout the entire record.

3.2. Tabulated relations between the ISMR and Indian Ocean Indices

3.2.1. Contingency tables. In addition to a standard multiple regression analysis, we used the method of contingency tables to examine the association between the categories of ISMR and all the indices mentioned above. To do that, all data (ISMR, NINO3, SSTDMI, and EQWIN) are ranked and classified into two or three categories as indicated below. The chosen diversification allows testing different relationship and offers a measure of sensitivity to the definition of categories. The tables are analyzed separately for El Niño, La Niña, and neutral years to show the influence of Indian Ocean indices separately for each situation. Here the El Niño years are defined as the years corresponding to the upper 33% of NINO3 values during the period of 1881–1998. La Niña years are those with the lower 33% of NINO3 values, and neutral years are the years with the middle 33% values.

The cases that we examined are shown in Table II. Variables are divided into three equal categories (tercile) or in halves, except for cases 1.1 and 2.1. In these two cases, the ISMR values are divided into two unequal categories; the lower 1/3 *vs* the upper 2/3 for case 1.1, and the lower 2/3 *vs* the upper 1/3 for case 2.1. Since there is a negative association between the ISMR and ENSO, there tends to be more events, overall, in the lower 33% of ISMR during El Niño years and in the upper 33% during La Niña years. The SSTDMI/EQWIN are also divided into two categories, but as the lower 50% and the upper 50%. In cases 1.2, 2.2, and 3.2, ISMR

DOI: 10.1002/joc

Table II. Categories for contingency tables of the EQWIN and ISMR. ENSO phases are separated into warmest 1/3 (El Niño), middle 1/3 (Neutral), and coldest 1/3 (La Niña) categories on the basis of NINO3 values. ISMR and SSTDMI/EQWIN are divided into categories as summarized in the third and fourth columns. The Fisher's exact test is applied except for the case 3.1. *P*-values that indicate significance level are calculated and the shaded rows are categories that show an association at more than the 90% significance level.

	ENSO	ISMR	EQWIN	Statistical test	*P*-value
Case 1.1	El Niño	Lower 33%, Upper 67%	Lower 50% Upper 50%	Fisher's exact	0.01
Case 1.2	El Niño	Lower 50%, Upper 50%	Lower 50% Upper 50%	Fisher's exact	0.01
Case 1.3	El Niño	Lower 33% Upper 33%	Lower 33% Upper 33%	Fisher's exact	0.09
Case 2.1	La Niña	Lower 67% Upper 33%	Lower 50% Upper 50%	Fisher's exact	0.28
Case 2.2	La Niña	Lower 50% Upper 50%	Lower 50% Upper 50%	Fisher's exact	0.57
Case 2.3	La Niña	Lower 33% Upper 33%	Lower 33% Upper 33%	Fisher's exact	0.21
Case 3.1	Neutral	Lower 33% Middle 33% Upper 33%	Lower 50% Upper 50%	Chi-squared	0.20
Case 3.2	Neutral	Lower 50%, Upper 50%	Lower 50% Upper 50%	Fisher's exact	0.06
Case 3.3	Neutral	Lower 33% Upper 33%	Lower 33% Upper 33%	Fisher's exact	0.13

and SSTDMI/EQWIN are divided into the lower 50% and upper 50%. In cases 1.3, 2.3, and 3.3, ISMR and SSTDMI/EQWIN are divided into terciles, but only the lower and upper 33% are taken as objects of analysis.

The numbers of events in each category are calculated and the association between the categories is tested. For 2×2 tables, we use Fisher's exact test, which calculates the exact probability distribution for a set of tables under the constraint of having the same row and column totals, and thus it is a non-parametric test. Since the calculation that is necessary for obtaining the exact probability distribution grows rapidly with the size of the contingency table, we use this non-parametric test only with 2×2 tables (See Appendix). For the 3×2 tables, we apply the parametric Chi-squared test as an approximation.

The results are consistent with the existence of a significant association between ISMR and EQWIN under certain ENSO conditions. Specifically, during the El Niño events, there is a negative association between the categories of EQWIN and ISMR (for case 1.1 with 99% significance, case 1.2 with 99% significance, and case 1.3 with 91% significance). However, during the neutral years, only one case shows a significant association between the categories of EQWIN and ISMR (case 3.2 with 94% significance). During the La Niña events, the dependencies between the categories of the ISMR and EQWIN are not significant ($p > 0.2$) in any of the cases. This ENSO-EQWIN-ISMR relationship is explored further in the next subsection. The contingency tables for cases 1.1, 2.1, and 3.1 are shown in Table III.

Table III. Contingency tables for the cases 1.1, 2.1, and 3.1. The numbers of events for each category are summarized.

Case 1.1, ENSO: El Niño

ISMR \ EQWIN	Below (50%)	Above (50%)	
Below (33%)	13	12	25
Above (66%)	13	1	14
	26	13	39

Case 2.1, ENSO: La Niña

ISMR \ EQWIN	Below (50%)	Above (50%)	
Below (66%)	4	12	16
Above (33%)	9	14	23
	13	26	39

Case 3.1, ENSO: Neutral

ISMR \ EQWIN	Below (50%)	Above (50%)	
Below (33%)	3	8	11
Normal (33%)	10	8	18
Above (33%)	7	4	11
	20	20	40

The same tables were formed with SSTDMI instead of EQWIN (tables not shown). During the El Niño

DOI: 10.1002/joc

events, there is a weak positive association for case 1.1 ($p = 0.29$) and case 1.2 ($p = 0.32$), but it is too weak to lead to any significant conclusion. Other phases of ENSO show an even weaker relationship. We obtained a similar result with the SSTDMI based on the Hadley Center SST anomaly data.

3.2.2. Scatterplots. The relationship between EQWIN and ISMR that was suggested by the contingency tables can also be seen in a scatterplot derived from the different index values. Figure 2 is similar to the one in Gadgil *et al*. (2004), but for the longer period studied here. It shows the relationship between ENSO, EQWIN, and ISMR. The dotted lines indicate the upper and lower 33% of each index. The excesses/deficits of ISMR are colored red/blue and separated by a line (curved dotted line in Figure 2) that is defined by the best ISMR regression model using NINO3 and EQWIN (model 4 of Table I).

During El Niño events (NINO3 in the upper 33%), the necessary (but not sufficient) condition for excess ISMR is a negative EQWIN (the lowest 33%). Between 1881 and 1998, there are 9 cases of excess (upper 33%) or normal (middle 33%) rainfall events out of 19 co-occurrences of El Niño and negative EQWIN; while the ISMR values are always deficient (bottom 33%) when both El Niño and positive EQWIN occur (eight events out of eight). The distribution is significantly different from random (see cases 1.1, 1.2, and 1.3 in Table II). During the La Niña events, there are 10 deficit or normal rainfall events out of 17 co-occurrences of La Niña and positive EQWIN, while rainfall tends to be in excess during co-occurrences of La Niña and negative EQWIN (six events out of seven). Thus, there seems to be the same negative association with EQWIN seen during the El Niño events, but the relationship is not clear enough to be statistically significant during La Niña.

3.2.3. Spatial distribution of the rainfall over India. A subject of interest is the spatial distribution of rainfall over India as a function of the indices we presented above. Figure 3 presents a composite map of the precipitation anomalies (from Hulme, 1992, 1994; Hulme *et al*., 1998) over India during El Niño, La Niña, and neutral years for the lower 50% minus the upper 50% of the EQWIN index. Only the regions where the differences are significant at a 90% or higher confidence level (based on a standard Student's t-test) are plotted. The differences between two composites are significant during El Niños in central and northern India. During neutral and La Niña years, the signals are less significant than during El Niños. The negative anomalies of the zonal wind over the equatorial Indian Ocean tend to be associated with increased rainfall in the east-central India (about 80°E, 25–28°N) during the neutral years and in southern India during La Niña, although the areas of significance are small.

Similar composite maps of the precipitation anomalies over India were made from the lower 50% minus the upper 50% of SSTDMI (figures are not shown here). The differences are not significant except in small regions for El Niño and La Niña cases. During the neutral years, eastern and southern India show increased rainfall when SSTDMI values fall in the lower 50%, which is contrary to the assumption suggested by Ashok *et al*. (2001, 2004).

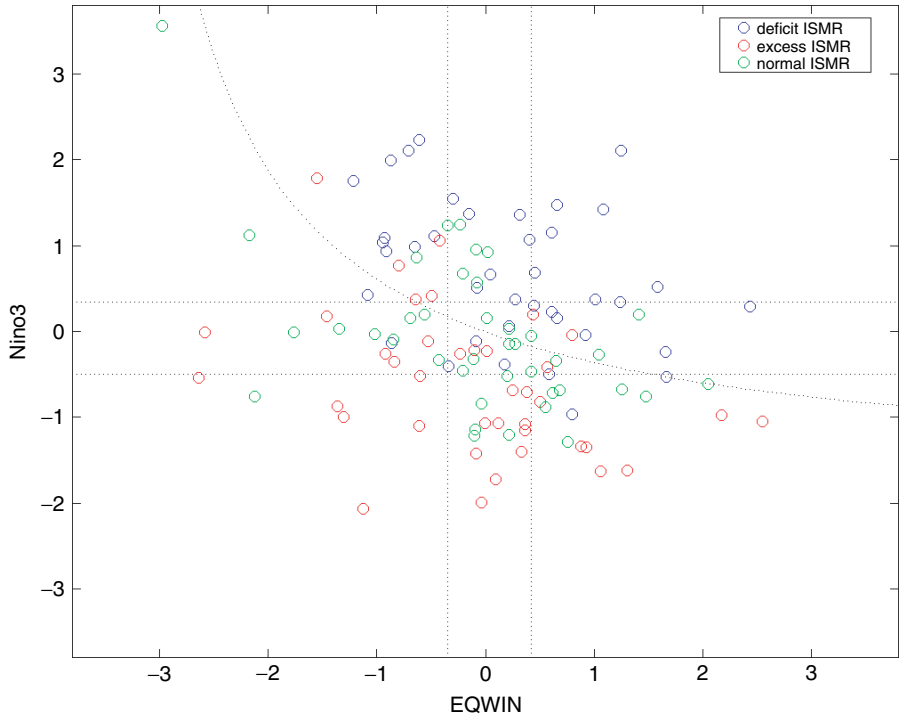

Figure 2. Scatterplot showing the relationship between EQWIN, NINO3 and ISMR. The blue/red/green dots indicate deficit/excess/normal ISMR values (based on tercile division). The dotted horizontal and vertical lines indicate the upper and lower 33% of each index. The curved dotted line defines the best ISMR reconstruction model (model 4, see Section 3.1 and Table I).

DOI: 10.1002/joc

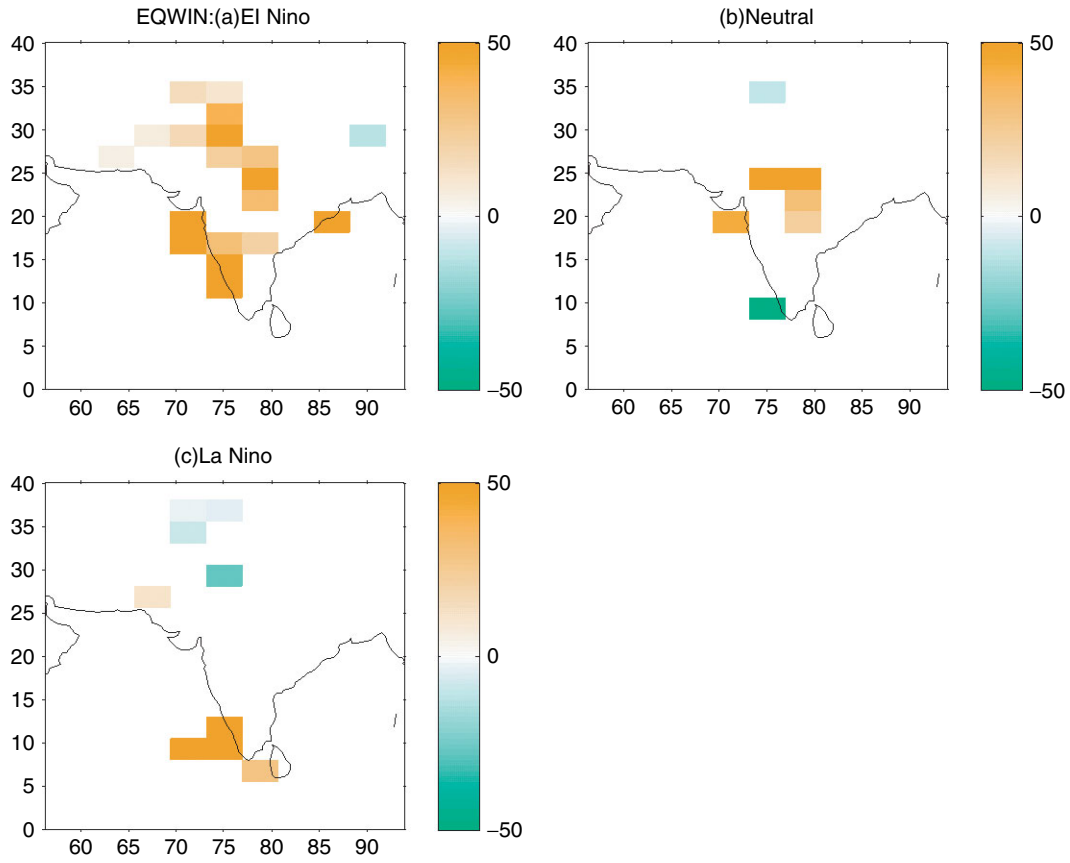

Figure 3. Composites of the mean JJAS rainfall anomaly (mm/month) during: (a) El Niño events with co-occurring negative EQWIN (the lower 50%) minus those events that co-occur with positive (the upper 50%) EQWIN. (b) Neutral years co-occurring with negative EQWIN minus those events that co-occur with positive EQWIN. (c) La Niña events co-occurring with negative EQWIN minus those events that co-occur with positive EQWIN. Only boxes with 90% confidence and higher from a student's *t*-test are plotted.

This local effect does not come across in our tabulation analysis with SSTDMI.

4. SUMMARY AND DISCUSSION

Using long data records (1881–1998), we demonstrated that atmospheric conditions over the Indian Ocean help explain the relationship between ENSO and ISMR. The results of a multiple regression analysis show that the ISMR is better associated with the conditions of the EQWIN and NINO3 indices than with NINO3 alone. In particular, there is a negative association between the ISMR and EQWIN during El Niño years. Negative zonal wind anomalies over the equatorial Indian Ocean are associated with normal or excess summer monsoon rainfall over India despite the presence of El Niño. This association is found to be highly significant by various methods during El Niño events, but the association during neutral and La Niña years is not coherent or significant.

Contingency tables show a significant association between various categories of ISMR and EQWIN during El Niño but not during La Niña years. The composite maps of land precipitations also indicate that this relationship is much more significant during El Niño events. On the other hand, the relationship between SSTDMI, the SST anomaly difference between the western and eastern Indian Ocean, and ISMR is weak and we cannot demonstrate a significant contribution of this SST pattern by any of the methods we used during the period analyzed.

Our results regarding the equatorial zonal wind anomalies are essentially consistent with the previous studies of Gadgil *et al*. (2003, 2004), which analyzed only the recent data record. Thus, it is possible to conclude that the association between the Indian Monsoon, equatorial zonal wind, and ENSO holds good for the entire observational record. However, the hypothesis regarding this 3-way link is only demonstrated with confidence during El Niño events. It is not clear why the behavior of EQWIN is not important during La Niña. Also, the contingency tables do not show strong association during neutral years and, as we have seen in our composites, the significant relationship between rainfall and EQWIN is limited to a certain small area of India. The limitation of observational data makes it difficult to further explore this issue.

On the basis of the above observation, we can only speculate regarding the physical mechanisms behind the association that we found in our study. One likely explanation lies in the nature of the region over which the EQWIN index was defined. In climatology, this is

DOI: 10.1002/joc

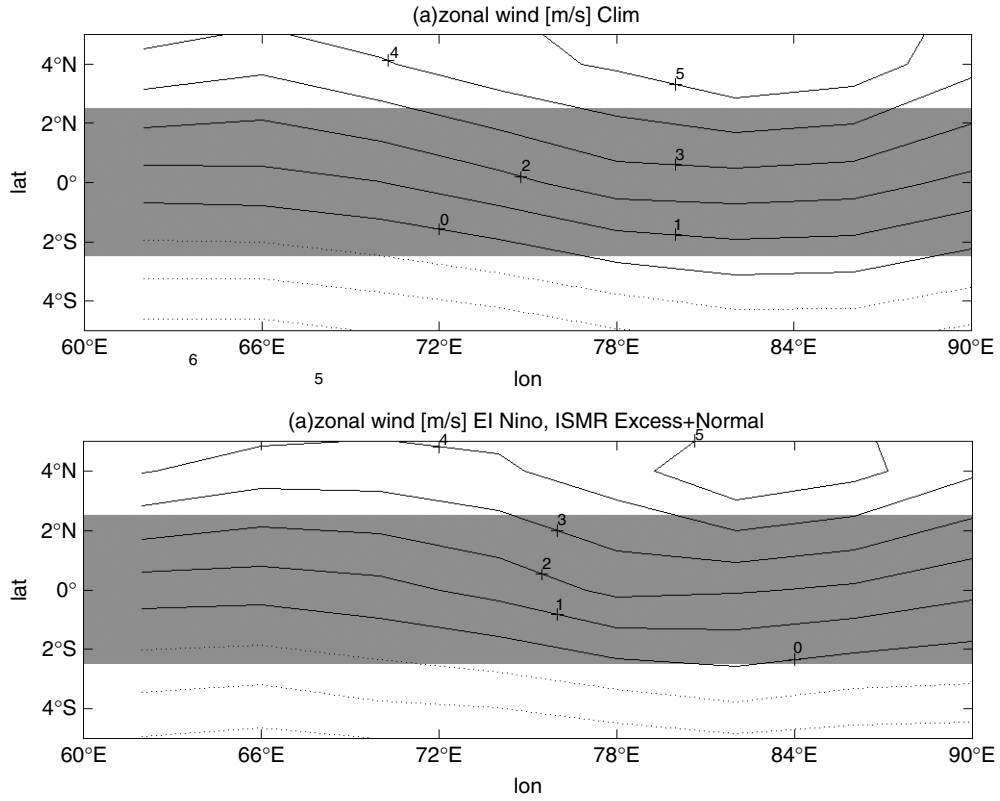

Figure 4. JJAS zonal wind. (a) Climatology, (b) during the co-occurrence of El Niño and normal and excess ISMR. The shaded box represents the region of EQWIN index. The solid line indicates the positive values and the dotted line indicates the negative values.

a transition zone between westerlies and easterlies. The negative EQWIN values that are associated with wetter ISMR during El Niño indicate the northward shift of the westerly wind belt and possibly the northward shift of the low-pressure center over India (see Figure 4). In such a relationship the change in EQWIN could be diagnostic rather than prognostic. Gadgil *et al*. (2003) proposed the physical mechanisms of the link between EQWIN and ISMR by referring to a change in deep convection based on the OLR data. This hypothesis cannot be verified in the same way over the longer period because OLR observations are not available for the period before 1979.

Identifying causality is the most challenging part of this research. We cannot conclude from our results that the negative anomalies of zonal wind over the equatorial Indian Ocean directly cause the enhanced rainfall over India; we can only conclude that negative EQWIN states tend to co-occur with enhanced rainfall during El Niño. In these cases, we could not find an association between the previous season EQWIN and ISMR. Moreover, sometimes the same EQWIN and ENSO index combinations yield different consequences of ISMR. For example, in the summer of 1982, a developing El Niño was associated with below normal ISMR. In the following year, El Niño decayed as ISMR was above normal. However, the four-month averaged ENSO and EQWIN indices were the same in both these years. The evolution phases of ENSO and EQUINOO are missed in the mean indices of the four months that we used in our study.

Because we have examined the data from more than one hundred years, we believe that our conclusions are robust and that we have been successful in capturing the relationship between the seasonal EQWIN and ISMR. As such, our study, identifying the association in the long-term record, is an important step in investigating the possibility of finding the relationship that is useful for ISMR prediction. Other issues that are related to the link between the monsoon and ENSO, including the decadal variability in the underlying state of the Indian Ocean (Allan *et al*., 1995) or, for that matter, changes in the characteristics of ENSO (Allan *et al*., 2003), are currently being pursued and will be addressed in a forthcoming paper.

ACKNOWLEDGEMENTS

We thank Dr. A. Kaplan for valuable comments regarding the data and Dr. S. Gadgil for a helpful discussion. CI and MAC were supported by the Cooperative Institute for Climate Applications and Research (CICAR) award number NA03OAR4320179 20A from the National Oceanic and Atmospheric Administration, U.S. Department of Commerce. YK was supported under NSF grant ATM-0347009. This is Lamont-Doherty Earth Observatory contribution number, 6960.

DOI: 10.1002/joc

APPENDIX: The Fisher's exact test (Conover, 1980)

	Column 1	Column 2	
Row 1	x	$r-x$	r
Row 2	$c-x$	$N-r-c+x$	$N-r$
	c	$N-c$	N

N observations are summarized in the table above, whose row and column totals are fixed. The exact distribution of the test statistics of this table is given by the hypergeometric distribution.

$$P(T_2 = x) = \frac{\binom{r}{x}\binom{N-r}{c-x}}{\binom{N}{c}} x \quad x = 0, 1, \ldots, \min(r, c)$$

$$= 0 \text{ for all other values of x}$$

Lower Tailed Test

$$H_0 : p_1 \geq p_2$$

$$H_1 : p_1 < p_2$$

where p_1 is the probability of an observation in row 1 being classified into column 1, p_2 is the probability of an observation in row 2 being classified into column 1, and t_{obs} is the observed value of T_2.

If $P(T_2 \leq t_{obs}) \leq \alpha$, reject H_0 at the level of significance α. Use this when there is a negative association between the variables.

Upper Tailed Test

$$H_0 : p_1 \leq p_2$$

$$H_1 : p_1 > p_2$$

If $P(T_2 \geq t_{obs}) \leq \alpha$, reject H_0 at the level of significance α. Use this when there is a positive association between the variables.

REFERENCES

Allan RJ, Lindesay JA, Reason CJC. 1995. Multidecadal variability in the climate system over the Indian-Ocean region during the austral summer. *Journal of Climate* **8**: 1853–1873.

Allan RJ, Reason CJC, Lindesay JA, Ansell TJ. 2003. Protracted ENSO episodes and their impacts in the Indian Ocean region. *Deep-Sea Research II* **50**(12): 2331–2347.

Ashok K, Guan Z, Yamagata T. 2001. Impact on the Indian Ocean dipole on the relationship between the Indian monsoon rainfall and ENSO. *Geophysical Research Letters* **28**: 4499–4502.

Ashok K, Guan Z, Saji NH, Yamagata T. 2004. On the individual and combined influences of the ENSO and the Indian Ocean dipole on the Indian summer monsoon. *Journal of Climate* **17**: 3141–3154.

Burnham KP, Anderson DR. 2003. *Model Selection and Multimodel Inference: A Practical Information-theoretic Approach*. Springer-Verlag: New York.

Conover WJ. 1980. *Practical Nonparametric Statistics*, 2nd edn. John Wiley and Sons: New York.

Gadgil S, Vinayachandran PN, Francis PA. 2003. Droughts of the Indian summer monsoon: role of clouds over the Indian Ocean. *Current Science* **85**(12): 1713–1719.

Gadgil Sulochana, Vinayachandran PN, Francis PA, Gadgil Siddhartha. 2004. Extremes of the Indian summer monsoon rainfall, ENSO and equatorial Indian Ocean oscillation. *Geophysical Research Letters* **31**(12): L12213.

Hulme M. 1992. A 1951–80 global land precipitation climatology for the evaluation of General Circulation Models. *Climate Dynamics* **7**: 57–72.

Hulme M. 1994. Validation of large-scale precipitation fields in General Circulation Models. In *Global Precipitations and Climate Change*, *NATO ASI Series*, Desbois M, Desalmand F (eds). Springer-Verlag: Berlin; , 466 387–406.

Hulme M, Osborn TJ, Johns TC. 1998. Precipitation sensitivity to global warming: comparison of observations with HadCM2 simulations. *Geophysical Research Letters* **25**: 3379–3382.

Kaplan A, Cane MA, Kushnir Y, Clement AC, Blumenthal MB, Rajagopalan B. 1998. Analyses of global sea surface temperature 1856–1991. *Journal of Geophysical Research-Oceans* **103**(C9): 18567–18589.

Kripalani RH, Kulkarni A. 1997. Climatic impact of El Nino/La Nina on the Indian monsoon: a new perspective. *Weather* **52**: 39–46.

Kripalani RH, Kumar P. 2004. Northeast monsoon rainfall variability over south peninsular India vis-à-vis the Indian Ocean dipole mode. *International Journal of Climatology* **24**(10): 1267–1282.

Kripalani RH, Oh J-H, Kang J-H, Sabade SS, Kulkarni A. 2005. Extreme monsoons over East Asia: possible role of Indian Ocean zonal mode. *Theoretical and Applied Climatology* **82**: 81–94.

Krishna Kumar K, Rajagopalan B, Cane MA. 1999. On the weakening relationship between the Indian monsoon and ENSO. *Science* **287**: 2156–2159.

Lau N-C, Nath MJ. 2000. Impact ENSO on the variability of the Asian-Australian Monsoons as simulated in GCM experiments. *Journal of Climate* **13**(24): 4287–4309.

Rasmusson EM, Carpenter TH. 1983. The relationship between eastern equatorial Pacific sea surface temperatures and rainfall over India and Sri Lanka. *Monthly Weather Review* **111**(3): 517–528.

Rayner NA, Parker DE, Horton EB, Folland CK, Alexander LV, Rowell DP, Kent EC, Kaplan A. 2003. Global analyses of SST, sea ice and night marine air temperature since the late nineteenth century. *Journal of Geophysical Research* **108**: D14,4407.

Reason CJC, Allan RJ, Lindesay JA, Ansell TJ. 2000. ENSO and climatic signals across the Indian Ocean Basin in the global context: part I, interannual composite patterns. *International Journal of Climatology* **20**(11): 1285–1327.

Ropelewski CF, Halpert MS. 1987. Global and regional scale precipitation patterns associated with the El Nino/Southern Oscillation. *Monthly Weather Review* **115**: 1606–1626.

Saha KR. 1970. Zonal anomaly of sea surface temperature in equatorial Indian Ocean and its possible effect upon monsoon circulation. *Tellus* **4**: 403–409.

Saji NH, Goswami BN, Vinayachandran PN, Yamagata T. 1999. A dipole mode in the tropical Indian Ocean. *Nature* **401**: 360–363.

Sakamoto Y, Ishiguro M, Kitagawa G. 1986. *Akaike Information Criterion Statistics*. KTK Scientific Publishers: Tokyo.

Sontakke NA, Pant GB, Singh N. 1993. Construction of all-India summer monsoon rainfall series for the period 1844–1991. *Journal of Climate* **6**: 1807–1811.

Wang B, Wu R, Li T. 2003. Atmosphere–warm Ocean interaction and its impacts on Asian–Australian monsoon variation. *Journal of Climate* **16**(8): 1195–1211.

Webster PJ, Yang S. 1992. Monsoon and ENSO: selectively interactive system. *Quarterly Journal of the Royal Meteorological Society* **118**: 877–926.

Webster PJ, Moore AM, Loschnigg JP, Leben RR. 1999. Coupled ocean–atmosphere dynamics in the Indian Ocean during 1997–98. *Nature* **401**: 356–360.

Worley SJ, Woodruff SD, Reynolds RW, Lubker SJ, Lott N. 2005. ICOADS release 2.1 data and products. *International Journal of Climatology* **25**: 823–842.

DOI: 10.1002/joc